

Solar neutrinos as probes of neutrino-matter interactions

Alexander Friedland*

Theoretical Division, T-8, MS B285, Los Alamos National Laboratory, Los Alamos, NM 87545

Cecilia Lunardini† and Carlos Peña-Garay‡

School of Natural Sciences, Institute for Advanced Study, Einstein Drive, Princeton, NJ 08540

(Dated: February 25, 2004)

Data from solar neutrino and KamLAND experiments have led to a discovery of nonzero neutrino masses. Here we investigate what these data can tell us about neutrino interactions with matter, including the poorly constrained flavor-changing $\nu_e - \nu_\tau$ interactions. We give examples of the interaction parameters that are excluded by the solar/KamLAND data and are beyond the reach of other experiments. We also demonstrate that flavor-changing interactions, at the allowed level, may profoundly modify the conversion probability for neutrinos of energy $\lesssim 6$ MeV and the values of the mass parameter inferred from the data. The implications for future experiments are discussed.

I. INTRODUCTION

In the Standard Model (SM), neutrinos are massless and interact by exchanging W and Z gauge bosons. For several decades, experiments have been trying to test this paradigm. Finally, a breakthrough has emerged: data from the solar, atmospheric, and reactor neutrino experiments have indicated that neutrinos are massive. At the moment, this remarkable result stands as the only solid evidence for physics beyond the SM. One of the pressing issues is to test the SM by accurately measuring the neutrino-matter interactions.

The aim of this Letter is to investigate what can be learned about neutrino-matter interactions from present and future solar and KamLAND neutrino data. We answer two questions: (i) Can the solar and KamLAND experiments constrain parts of the parameter space that are presently inaccessible by non-oscillation experiments? (ii) Can the uncertainty in our present knowledge of neutrino-matter interactions affect the determination of the oscillation parameters? As we show, the answer to both questions is affirmative. We give explicit examples of parameters that are disfavored by solar and KamLAND data and that are beyond the reach of non-oscillation experiments. We also demonstrate that non-standard interactions (NSI), at an allowed level, can qualitatively modify the fit to the data and change the values of inferred mass parameters. This scenario leads to non-trivial predictions for future experiments. A full presentation of the numerical constraints we obtain is beyond the scope of this Letter and will be given elsewhere [1].

Oscillations of massive solar neutrinos in the presence of the NSI have been extensively studied [2, 3, 4], with an emphasis on the limit of small flavor-changing interactions. We extend the formalism developed in these papers to make it applicable to our problem.

II. NSI AND SOLAR NEUTRINOS: THE PHYSICS

Low-energy neutrino interactions can be described by four-fermion interaction vertices, $L \ni \sum \bar{\psi}\psi\bar{\psi}\psi$. The vertices affecting neutrino evolution in matter are those containing two neutrino lines (2ν). In the SM, these vertices receive contributions from neutral current (NC) processes and, if the initial state contains a charged lepton, also charged current (CC) processes. The NC processes are predicted to be flavor-preserving and universal. Possible non-standard (both flavor-preserving and flavor-changing) contributions to the 2ν vertices can, most generally, be parameterized as

$$L^{NSI} = -2\sqrt{2}G_F(\bar{\nu}_\alpha\gamma_\rho\nu_\beta)(\epsilon_{\alpha\beta}^{f\bar{f}L}\bar{f}_L\gamma^\rho\tilde{f}_L + \epsilon_{\alpha\beta}^{f\bar{f}R}\bar{f}_R\gamma^\rho\tilde{f}_R) + h.c. \quad (1)$$

Here $\epsilon_{\alpha\beta}^{f\bar{f}L}$ ($\epsilon_{\alpha\beta}^{f\bar{f}R}$) denotes the strength of the NSI between the neutrinos ν of flavors α and β and the left-handed (right-handed) components of the fermions f and \tilde{f} ; G_F is the Fermi constant.

Bounds on the epsilons come from accelerator-based experiments, such as NuTeV [5] and CHARM [6], and experiments involving charged leptons. In the later case, we do not include bounds obtained by the $SU(2)$ symmetry, since strictly speaking these can be avoided if, for example, the corresponding operators contain Higgs doublets [7]. Both types of experiments are quite effective at constraining the vertices involving the muon neutrino, $\epsilon_{e\mu} \lesssim 10^{-3}$, $\epsilon_{\mu\mu} \lesssim 10^{-3} - 10^{-2}$. At the same time, bounds on ϵ_{ee} , $\epsilon_{e\tau}$, and $\epsilon_{\tau\tau}$ are rather loose, e.g., $|\epsilon_{\tau\tau}^{uuR}| < 3$, $-0.4 < \epsilon_{ee}^{uuR} < 0.7$, $|\epsilon_{\tau e}^{uu}| < 0.5$, $|\epsilon_{\tau e}^{dd}| < 0.5$ [8].

NSI can modify both the neutrino propagation (oscillation) and neutrino detection processes. The propagation effects of NSI are, first of all, only sensitive to $\epsilon_{\alpha\beta}^{f\bar{f}}$ when $f = \tilde{f}$ [36] (henceforth, $\epsilon_{\alpha\beta}^{f\bar{f}P} \equiv \epsilon_{\alpha\beta}^{fP}$), and, second, only to the vector component of that interaction, $\epsilon_{\alpha\beta}^f \equiv \epsilon_{\alpha\beta}^{fL} + \epsilon_{\alpha\beta}^{fR}$. The matter piece of the oscillation Hamiltonian can be written (up to an irrelevant constant)

*Electronic address: friedland@lanl.gov

†Electronic address: lunardi@ias.edu

‡Electronic address: penya@ias.edu

as:

$$H_{\text{mat}}^{3 \times 3} = \sqrt{2} G_F n_e \begin{pmatrix} 1 + \epsilon_{ee} & \epsilon_{e\mu}^* & \epsilon_{e\tau}^* \\ \epsilon_{e\mu} & \epsilon_{\mu\mu} & \epsilon_{\mu\tau}^* \\ \epsilon_{e\tau} & \epsilon_{\mu\tau} & \epsilon_{\tau\tau} \end{pmatrix}, \quad (2)$$

where n_e is the number density of electrons in the medium. The epsilons here are the sum of the contributions from electrons (ϵ^e), up quarks (ϵ^u), and down quarks (ϵ^d) in matter: $\epsilon_{\alpha\beta} \equiv \sum_{f=u,d,e} \epsilon_{\alpha\beta}^f n_f / n_e$. Hence, unlike in the standard case ($\epsilon_{\alpha\beta} = 0$), the NSI matter effects depend on the chemical composition of the medium.

The CC detection reactions at SNO, KamLAND and the radiochemical experiments, just like the production reactions in the Sun, are unchanged by Eq. (1). On the other hand, the neutrino-electron elastic scattering (ES) reactions at Super-Kamiokande and SNO, and the NC reaction at SNO could be affected. The SNO NC reaction is mostly an axial current process [9], while the ES reaction depends on both axial and vector parts. Hence, the former is independent of the oscillation Hamiltonian (2), while the latter is not.

Since both $\epsilon_{e\mu}$ and $\epsilon_{\mu\mu}$ are strongly constrained, we set them to zero and vary ϵ_{ee} , $\epsilon_{e\tau}$, $\epsilon_{\tau\tau}$. Even with this reduction, the parameter space of the problem is quite large: different assignment of the diagonal and offdiagonal NSI to electrons, and u and d quarks yield different dependences of the oscillation Hamiltonian on the chemical composition and different detection cross sections. To avoid complicating our main point with technical details, we limit our study to the case of NSI on quarks, assigning the same strength to the interaction with u and d quarks.

For the solar neutrino analysis, we perform the standard reduction of the 3×3 Hamiltonian to a 2×2 Hamiltonian. This involves performing a rotation in the $\mu - \tau$ subspace by the atmospheric angle θ_{23} and taking the first two columns/rows. This simplification is valid if (i) the $1 - 3$ mixing angle is small: $\theta_{13} \ll 1$ and (ii) $G_F n_e \epsilon_{e\tau} \ll \Delta m_{\text{atm}}^2 / (2E_\nu)$, with E_ν being the neutrino energy and Δm_{atm}^2 the difference of the squared masses, $\Delta m_{\text{atm}}^2 \equiv m_3^2 - m_2^2$, as given by atmospheric neutrino data. The first requirement is ensured by the experimental bound from CHOOZ [10]; the second one can be checked to hold even for $\epsilon_{e\tau}$ of order unity. The vacuum oscillation Hamiltonian then takes the usual form

$$H_{\text{vac}} = \begin{pmatrix} -\Delta \cos 2\theta & \Delta \sin 2\theta \\ \Delta \sin 2\theta & \Delta \cos 2\theta \end{pmatrix}, \quad (3)$$

where $\Delta \equiv \Delta m^2 / (4E_\nu)$ and Δm^2 is the mass splitting between the first and second neutrino mass states: $\Delta m^2 \equiv m_2^2 - m_1^2$. The matter contribution can be written (once again, up to an irrelevant overall constant) as:

$$H_{\text{mat}}^{\text{NSI}} = \frac{G_F n_e}{\sqrt{2}} \begin{pmatrix} 1 + \epsilon_{11} & \epsilon_{12}^* \\ \epsilon_{12} & -1 - \epsilon_{11} \end{pmatrix}, \quad (4)$$

where the quantities ϵ_{ij} ($i = 1, 2$) depend on the original epsilons and on the rotation angle θ_{23} :

$$\epsilon_{11} = \epsilon_{ee} - \epsilon_{\tau\tau} \sin^2 \theta_{23}, \quad \epsilon_{12} = -2 \epsilon_{e\tau} \sin \theta_{23}. \quad (5)$$

In Eq. (5) small corrections of order $\sin \theta_{13}$ or higher have been neglected. We introduce a useful parameterization:

$$H_{\text{mat}}^{\text{NSI}} = \begin{pmatrix} A \cos 2\alpha & A e^{-2i\phi} \sin 2\alpha \\ A e^{2i\phi} \sin 2\alpha & -A \cos 2\alpha \end{pmatrix}. \quad (6)$$

Here the parameters A , α and ϕ are defined as follows:

$$\begin{aligned} \tan 2\alpha &= |\epsilon_{12}| / (1 + \epsilon_{11}), & 2\phi &= \text{Arg}(\epsilon_{12}), \\ A &= G_F n_e \sqrt{[(1 + \epsilon_{11})^2 + |\epsilon_{12}|^2] / 2}. \end{aligned} \quad (7)$$

In absence of NSI we have $A = G_F n_e / \sqrt{2}$, $\alpha = 0$ and the Hamiltonian (6) reduces to its standard form.

Notice the appearance of the phase ϕ in Eq. (6). Since the phases of the basis states are chosen to make the elements in Eq. (3) real, ϕ cannot be *simultaneously* removed. This has been noted in the studies of terrestrial neutrino beams [11, 12], but overlooked in the solar neutrino literature.

What is the physical range for the parameters θ , α and ϕ ? In the standard case $\alpha = 0$, the physical range of θ is $[0, \pi/2]$, including the so-called ‘‘light’’ and ‘‘dark’’ sides [13]. A generalization to the NSI case is

$$\theta \in [0, \pi/2], \quad \alpha \in [0, \pi/2], \quad \phi \in [-\pi/2, \pi/2]. \quad (8)$$

These ranges of parameters cover all possibilities in Eqs. (3,6). For solar neutrinos, the range of ϕ could be cut in half, since points with ϕ and $-\phi$ give the same probability P_{ee} that a ν_e produced in the Sun is seen as a ν_e in a detector. Moreover, the points (θ, α, ϕ) and $(\pi/2 - \theta, \pi/2 - \alpha, \phi)$ are related by $P_{ee} \leftrightarrow P_{\mu\mu}$, which are equal in the 2-neutrino case by unitarity.

Let us determine the expression for P_{ee} . We first note that, because KamLAND selects $\Delta m^2 \gtrsim 10^{-5} \text{ eV}^2$, coherence between the Hamiltonian eigenstates is completely lost once one integrates over the neutrino energy spectrum and the neutrino production region in the Sun. The expression for the incoherent survival probability P_{ee} can be most easily derived in the basis that diagonalizes the matter Hamiltonian (6). We obtain the familiar form

$$P_{ee} = [1 + (1 - 2P_c) \cos 2\theta_\odot \cos 2\theta] / 2, \quad (9)$$

where θ_\odot is the mixing angle at the neutrino production point in the solar core and P_c is the level crossing probability. These quantities contain all the effects of the NSI. The angle θ_\odot is given by

$$\cos 2\theta_\odot = \frac{\cos 2\theta - x_\odot \cos 2\alpha}{\sqrt{1 + x_\odot^2 + 2x_\odot \cos 2\theta_{\text{rel}}}}, \quad (10)$$

$$\cos 2\theta_{\text{rel}} \equiv \sin 2\theta \sin 2\alpha \cos 2\phi - \cos 2\theta \cos 2\alpha. \quad (11)$$

Here $x_\odot \equiv A / \Delta$ at the neutrino production point.

The expression for P_c is also easily found in the same basis, where it becomes apparent that the dynamics of conversion in matter depends only on the relative orientation of the eigenstates of the vacuum and matter Hamiltonians. This allows to apply directly the known analytical solutions for P_c , and, upon rotating back, obtain a

generalization of these results to the NSI case. For example, the answer for the infinite exponential profile [14, 15] $A \propto \exp(-r/r_0)$ becomes $P_c = (\exp[\gamma(1 - \cos 2\theta_{\text{rel}})/2] - 1)/[\exp(\gamma) - 1]$, where $\gamma \equiv 4\pi r_0 \Delta = \pi r_0 \Delta m^2/E_\nu$. We further observe that since $\gamma \gg 1$ the adiabaticity violation occurs only when $|\theta - \alpha| \ll 1$ and $\phi \simeq \pi/2$, which is the analogue of the small-angle MSW [16] effect in the rotated basis. The range of solar densities for which level jumping can take place is narrow, defined by $A \simeq \Delta$ [17]. If a neutrino is produced at a lower density, its evolution is adiabatic, while if it is produced at a higher density, the level crossing probability P_c is given to very good accuracy by the formula for the linear profile, with an appropriate gradient taken along the neutrino trajectory,

$$P_c \simeq \Theta(A - \Delta)e^{-\gamma(\cos 2\theta_{\text{rel}}+1)/2}, \quad (12)$$

where $\Theta(x)$ is the step function, $\Theta(x) = 1$ for $x > 0$ and $\Theta(x) = 0$ otherwise. We emphasize that our results differ from the similar ones given in [4, 18] in three important respects: (i) they are valid for all, not just small values of α (which is essential for our application), (ii) they include the angle ϕ , and (iii) the argument of the Θ function does not contain $\cos 2\theta$, as follows from [17]. We stress that for large values of α and $\phi \simeq \pi/2$ adiabaticity is violated for large values of θ .

Finally, to get an idea on the size of the day/night asymmetry, $A_{\text{DN}} \equiv 2(N - D)/(N + D)$, (here D (N) denotes the ν_e flux at the detector during the day (night)) we can model the Earth as a sufficiently long (compared to the oscillation length) object of constant density. For ${}^8\text{B}$ neutrino energies, this is appropriate for $\Delta m^2 \gtrsim 3 - 5 \cdot 10^{-5} \text{ eV}^2$. Introducing a small parameter $x_\oplus \equiv A/\Delta$, where A is evaluated for a typical density inside the Earth, we find, to the first order in x_\oplus ,

$$A_{\text{DN}} \simeq x_\oplus \frac{\sin 2\theta(\cos 2\alpha \sin 2\theta + \cos 2\phi \sin 2\alpha \cos 2\theta)}{-[\cos 2\theta_\odot(1 - 2P_c)]^{-1} - \cos 2\theta}. \quad (13)$$

We find that Eq. (13) gives a good agreement with precise numerical calculations for $n_e \simeq 1.6 \text{ moles/cm}^3$. For the lower Δm^2 region allowed by KamLAND, $\Delta m^2 \gtrsim 1 - 3 \cdot 10^{-5} \text{ eV}^2$, the oscillation length is comparable to the size of the Earth, however, the averaging in Eq. (13) still applies to a signal integrated over the zenith angle.

In Fig. 1 we plot the neutrino survival probability as a function of energy for several representative values of the NSI parameters. We take Δm^2 and θ corresponding to the best-fit LMA point and choose the production point to be at $r = 0.1R_\odot$. Curve (1) is the standard interaction case, given for reference. The other three curves represent the three qualitatively different regimes that are of interest to us. In the following we illustrate them in connection with observations. For definiteness, we consider real values of ϵ_{12} , both positive ($\phi = 0$) and negative ($\phi = \pi/2$). As is clear from Eq. (6), complex values ($0 < \phi < \pi/2$) interpolate between these two cases.

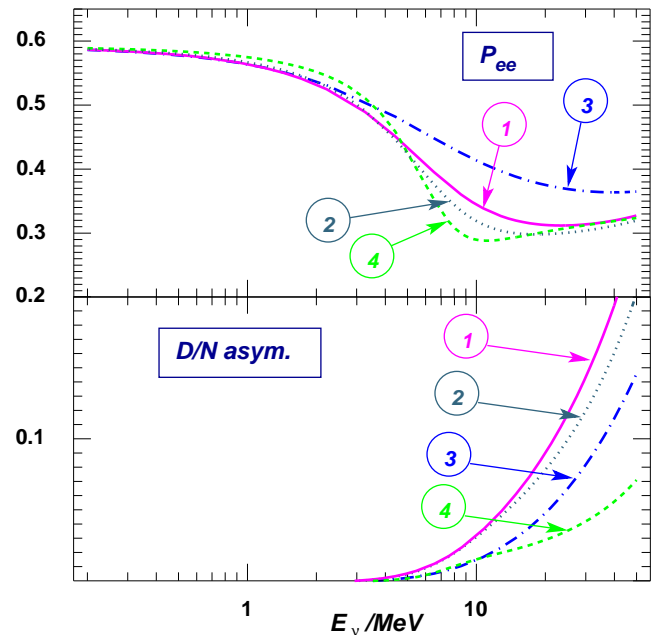


FIG. 1: The electron neutrino survival probability and the day/night asymmetry as a function of energy for $\Delta m^2 = 7 \times 10^{-5} \text{ eV}^2$, $\tan^2 \theta = 0.4$ and several representative values of the NSI parameters: (1) $\epsilon_{11}^u = \epsilon_{11}^d = \epsilon_{12}^u = \epsilon_{12}^d = 0$; (2) $\epsilon_{11}^u = \epsilon_{11}^d = -0.008$, $\epsilon_{12}^u = \epsilon_{12}^d = -0.06$; (3) $\epsilon_{11}^u = \epsilon_{11}^d = -0.044$, $\epsilon_{12}^u = \epsilon_{12}^d = 0.14$; (4) $\epsilon_{11}^u = \epsilon_{11}^d = -0.044$, $\epsilon_{12}^u = \epsilon_{12}^d = -0.14$. Recall that the parameters in Eq. (5) equal $\epsilon_{ij} = \epsilon_{ij}^u n_u/n_e + \epsilon_{ij}^d n_d/n_e$.

III. ANALYSIS OF DATA

We now turn to the comparison of the NSI predictions with observations. To do this, we perform a best fit analysis of the solar neutrino and KamLAND data along the lines of Refs. [19, 20]. In particular, solar data include the radiochemical rates [21, 22, 23, 24], the SK ES zenith-spectra [25], the SNO day-night spectra [26, 27, 28] measured in phase-I and the SNO rates measured in phase-II [29]. For consistency, the NC rate prediction for SNO is treated as a free parameter because it is affected by an unknown change in the axial coupling of the quarks that could accompany the vector NSI considered in our analysis. In our calculations, we use the updated BP04 [30] Standard Solar Model (SSM) fluxes, electron density and neutrino production point distributions in the Sun. For KamLAND we considered the measured antineutrino spectrum with visible energies higher than 2.6 MeV [31].

The key ingredients of our analysis turns out to be the rates and energy spectrum data from SNO and Super-Kamiokande. A comparison of the SNO CC rate with the Super-Kamiokande rate [26] and the SSM indicates that, within the energy range accessible for the two experiments, the electron neutrino survival probability is about 30%. No other distinguishing features, such as a day/night asymmetry or spectral distortion, are seen at

a statistically significant level [28]. In the case of the SM interaction, this turn out to be a very restrictive condition; as seen in Fig. 1, the range of energies for which the survival probability is constant at 30% (henceforth, “the flat window”) is barely large enough to cover the SNO energy window. On the low-energy end, the resonant condition in the solar core increases the neutrino survival probability; on the high-energy end, the resonant condition in the earth causes a large D/N effect. Hence, values of the NSI parameters that “shrink” the flat window, or shift it in the region disfavored by KamLAND, can be excluded. Conversely, if NSI increase the size of the flat window, new solutions may emerge.

A. $\epsilon_{12} > 0$

A typical behavior for this case is exhibited by curve (3): the “step” in P_{ee} becomes longer and the day/night asymmetry is not much smaller than in the SM case. These features point to a possible conflict with data. Our analysis confirms this expectation: a parameter scan [1] for $\epsilon_{12} > 0$ reveals that a significant fraction of the parameter space which is allowed by the accelerator-based data can be excluded by the solar/KamLAND data. As an example, we find that points with $\epsilon_{11} = 0$ and $\epsilon_{12}^u > 0.14$ (here and later, $\epsilon_{\alpha\beta}^u = \epsilon_{\alpha\beta}^d$ is assumed) are unacceptable at 90% confidence level (C.L.). If we keep A in the core of the Sun (at $r = 0.05R_{\odot}$) fixed to its standard value, $A = G_F n_e / \sqrt{2}$, we exclude points with $\epsilon_{12}^u > 0.11$ at the same C.L. (for 1 degree of freedom, dof, unless specified otherwise). The accelerator experiments allow values of order unity (in absolute value) for this parameter [8]. We stress that the latter probe only $|\epsilon_{12}|$, while, as we show here, oscillation experiments are sensitive to the complex phase ϕ (or, for real epsilons, to the sign of ϵ_{12}).

B. $\epsilon_{12} < 0$

For ϵ_{12} close to zero ($-0.08 \lesssim \epsilon_{12}^u < 0$), the only effect of the NSI is to flatten the part of the P_{ee} curve around 5-6 MeV, as illustrated by curve (2) in Fig. 1. No new solutions appear and the allowed region in the θ - Δm^2 plane is similar to that obtained with the SM interactions. This scenario has important implications for SNO, which can probe it by lowering its energy threshold.

Finally, curve (4), obtained for $\epsilon_{11}^u = -0.044$, $\epsilon_{12}^u = -0.14$, represents a novel and very interesting physical possibility. Its main feature is a significantly wider flat window, compared to the standard case. The key reason is the suppression of the day/night asymmetry on the high-energy end of the window. The physics of the suppression can be understood from Eq. (13), which, for $\phi = \pi/2$, gives $A_{DN} \propto \sin(2\theta - 2\alpha)$. If the parameters are chosen in such a way that θ and α in the Earth are comparable, the Earth regeneration effect is suppressed.

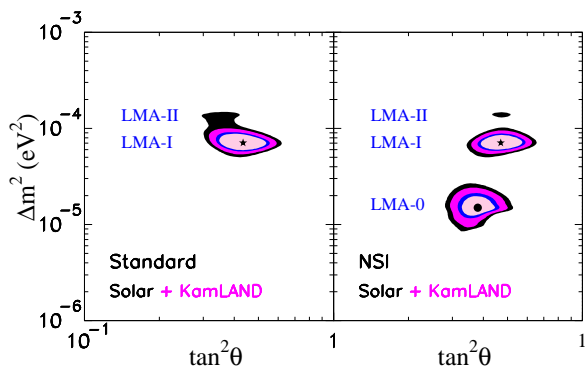


FIG. 2: Regions of Δm^2 and $\tan^2 \theta$ allowed at 90, 95, 99, 99.73% C.L. (2 dof) for SM interactions (left) and the NSI scenario (right) described by Eqs. (3-6). For the latter we used $\epsilon_{11}^u = \epsilon_{11}^d = -0.065$, $\epsilon_{12}^u = \epsilon_{12}^d = -0.15$.

Because of the difference in chemical composition, the difference $\theta - \alpha$ is larger in the Sun and, consequently, the evolution in the Sun is still adiabatic.

A broader flat window allows the fit region to extend to lower values of Δm^2 compared to the standard case. While KamLAND excludes the middle part of the new region, the bottom part of that region ($\Delta m^2 \sim (1 - 2) \times 10^{-5}$ eV²) is, in fact, allowed [20, 31]. Thus, in addition to the usual two solutions, LMA-I and LMA-II, a completely new disconnected solution emerges, which we shall denote LMA-0.

The situation is illustrated in Fig. 2, in which we compare the allowed regions in the standard case to those computed for chosen values of the NSI parameters: $\epsilon_{11}^u = -0.065$, $\epsilon_{12}^u = -0.15$. The best-fit point in the LMA-0 region has $\Delta m^2 = 1.5 \times 10^{-5}$ eV² and $\tan^2 \theta = 0.39$, with $\chi^2 = 81.7$. For the same NSI parameters, the χ^2 has another minimum, $\chi^2 = 79.9$, at $\Delta m^2 = 7.1 \times 10^{-5}$ eV² and $\tan^2 \theta = 0.47$, corresponding to the LMA-I solution. The two solutions, LMA-0 and LMA-I give comparably good fit; if only the KamLAND rate, and not spectrum, information is used, the LMA-0 fit is a bit better ($\chi^2 = 73.0$, against $\chi^2 = 73.7$ for the minimum in the LMA-I region). For comparison, the best fit parameters for the standard case are $\Delta m^2 = 7.1 \times 10^{-5}$ eV² and $\tan^2 \theta = 0.43$, with $\chi^2 = 79.6$ (using the KamLAND spectrum).

We note that the LMA-0 solution requires that the value of the ϕ angle be not too different from $\pi/2$. Numerically, if we fix all the other parameters to the values of fig. 2 and vary ϕ , we find that LMA-0 disappears at 90% C.L. for $\phi < 0.45\pi$. As ϕ is decreased further, the goodness of the overall fit decreases. Indeed, for $\phi = 0$ (positive ϵ_{12}), the survival probability has the features of curve (3) in Fig. 1, which are disfavored, as discussed earlier. The LMA-I solution disappears at 90% C.L. for $\phi < 0.31\pi$. A scan over the region of ϵ_{12} real and negative gives exclusion of regions of the parameter space allowed by accelerator limits. For instance, points with $\epsilon_{11} = 0$ and $\epsilon_{12}^u < -0.32$ are unacceptable at 90% C.L.

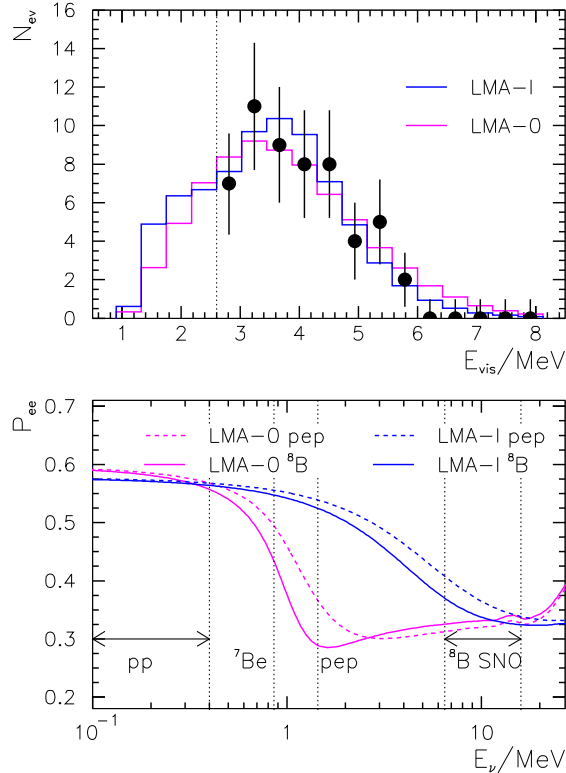


FIG. 3: The predicted KamLAND spectrum (top) and the time-averaged solar neutrino survival probability (bottom) for the LMA-0 best-fit point. For comparison, the standard LMA-I survival probability is also given. Refer to the text for details.

For A fixed to the standard value $G_F n_e / \sqrt{2}$ in the solar core, the limit is $\epsilon_{12}^u < -0.19$, at 90% C.L.

Our choice of $\epsilon_{12}^u = -0.15$ implies $\epsilon_{e\tau}^u = \epsilon_{e\tau}^{uL} + \epsilon_{e\tau}^{uR} \simeq 0.11$ (see Eq. (5)), i.e., for example, $\epsilon_{e\tau}^{uL} \simeq \epsilon_{e\tau}^{uR} \sim 0.05$. This about one order of magnitude smaller than the direct bound from CHARM [8]. A more interesting question is whether the NSI parameters of interest for the LMA-0 scenario could be tested with atmospheric neutrinos. For our specific case, the existing two-neutrino analyses [32, 33] do not provide an answer, as the problem is essentially a three-flavor one. Our investigation [1] shows that regions exist in the space of the NSI parameters where the effect of NSI on the atmospheric neutrino observables is minimal and a satisfactory fit to the data is obtained. As an example, a point in this allowed region is $\epsilon_{ee}^u = \epsilon_{ee}^d = -0.025$, $\epsilon_{e\tau}^u = \epsilon_{e\tau}^d = 0.11$, $\epsilon_{\tau\tau}^u = \epsilon_{\tau\tau}^d = 0.08$.

The survival probabilities for the best-fit point of the LMA-0 solution and the standard LMA-I solution are illustrated in Fig. 3 (bottom). The curves shown represent probabilities averaged over time and over the production region inside the Sun for the ${}^8\text{B}$ and pep components of the solar neutrino spectrum according to [30]. The prob-

abilities for ${}^7\text{Be}$ and pp neutrinos, not shown, are very close (with less than $\sim 7\%$ difference) to those for ${}^8\text{B}$ and pep respectively in the energy range of these neutrino fluxes. The energy intervals relevant to the different spectral components are also shown in the figure. The interval for ${}^8\text{B}$ neutrinos is cut from below at $E_\nu = 6.5$ MeV; this approximately corresponds to the threshold of $T \simeq 5$ MeV in the electron energy at the SNO experiment.

Interestingly, the LMA-0 solution has the features sought after in [34], where a sterile neutrino was introduced to eliminate the LMA-I upturn at SNO and improve the agreement with the Homestake rate.

It is remarkable that, despite the wealth of data collected up to this point, such radically different scenarios as LMA-0 and LMA-I cannot be distinguished. The data expected in the next several years, on the other hand, should be able to resolve the ambiguity. First, if the SNO experiment lowers its energy threshold, it may be able, with sufficient statistics, to look for the upturn expected for the LMA-I solution. The absence of the upturn would indicate the presence of NSI, or some other new physics. Second, the expected ${}^7\text{Be}$ flux in the case of LMA-0 is lower, and the difference could be detected by the Borexino experiment (or by the future solar phase of KamLAND). Third, the small value of Δm^2 could be detected in the KamLAND spectrum data. The predicted spectra for LMA-I (standard interactions) and LMA-0 are shown in Fig. 3 (top). It can be seen that the two are different at high energy where LMA-0 predicts more events. Thus, to make the discrimination it is necessary to both collect enough data and have a reliable calculation of the antineutrino flux for $E_{\bar{\nu}} \gtrsim 6$ MeV. Finally, as evident from Fig. 3, the two solutions make dramatically different predictions for a pep experiment[37].

While an observation consistent with the standard LMA-I solution would allow placing a very effective constraint on the neutrino-matter interactions, a discovery of a deviation consistent with the NSI signal would have truly profound particle physics implications. For example, according to Refs. [7, 8], such interaction could be due to the operator of the form $M^{-4} \bar{l}_R (H^\dagger \vec{\sigma} L) (\vec{L} \vec{\sigma} H) l_R \propto v^2 M^{-4} (\bar{\nu} \nu) (\bar{l}_R l_R)$. For this operator to have an effect on the solar neutrino survival probability, the coefficient $\propto v^2 M^{-4}$ must not be too small, i.e., the scale of new physics M must not be much higher than the weak scale (Higgs vev v). Thus, by looking for the NSI signatures in solar/reactor neutrinos the experiments could in fact be probing new physics at the TeV scale.

In summary, the present-day loose bounds on some of the neutrino interaction parameters introduce a serious uncertainty in the value of Δm^2 extracted from solar and KamLAND data, allowing for a new, disconnected solution. These uncertainties might be eliminated in the next several years, as more data are collected and analyzed by solar and KamLAND experiments. The nontrivial constraints on the neutrino interactions that can be derived from the present data will be further extended. On the

other hand, deviations from the SM neutrino interactions could indicate the presence of radically new physics. We urge experimentalists to consider these points in their data analysis.

A. F. was supported by the Department of Energy, under contract W-7405-ENG-36; C. L. and C. P.-G. were supported by a grant-in-aid from the W.M. Keck Foundation and the NSF PHY-0070928.

-
- [1] A. Friedland, C. Lunardini, and C. Peña-Garay, in preparation.
- [2] V. D. Barger, R. J. N. Phillips, and K. Whisnant, *Phys. Rev.* **D44**, 1629 (1991).
- [3] G. L. Fogli and E. Lisi, *Astropart. Phys.* **2**, 91 (1994).
- [4] S. Bergmann, *Nucl. Phys.* **B515**, 363 (1998).
- [5] G. P. Zeller *et al.* [NuTeV Collaboration], *Phys. Rev. Lett.* **88**, 091802 (2002) [Erratum-*ibid.* **90**, 239902 (2003)] [arXiv:hep-ex/0110059].
- [6] P. Vilain *et al.* [CHARM-II Collaboration], *Phys. Lett. B* **335**, 246 (1994).
- [7] Z. Berezhiani and A. Rossi, *Phys. Lett.* **B535**, 207 (2002), hep-ph/0111137.
- [8] S. Davidson, C. Peña-Garay, N. Rius, and A. Santamaria, *JHEP* **03**, 011 (2003), hep-ph/0302093.
- [9] T. W. Donnelly, D. Hitlin, M. Schwartz, J. D. Walecka, and S. J. Wiesner, *Phys. Lett.* **B49**, 8 (1974).
- [10] M. Apollonio *et al.* (CHOOZ), *Phys. Lett.* **B420**, 397 (1998), hep-ex/9711002.
- [11] M. C. Gonzalez-Garcia, Y. Grossman, A. Gusso, and Y. Nir, *Phys. Rev.* **D64**, 096006 (2001), hep-ph/0105159.
- [12] M. Campanelli and A. Romanino, *Phys. Rev.* **D66**, 113001 (2002), hep-ph/0207350.
- [13] A. de Gouvea, A. Friedland, and H. Murayama, *Phys. Lett.* **B490**, 125 (2000), hep-ph/0002064.
- [14] S. Toshev, *Phys. Lett.* **B196**, 170 (1987).
- [15] S. T. Petcov, *Phys. Lett.* **B200**, 373 (1988).
- [16] L. Wolfenstein, *Phys. Rev. D* **17**, 2369 (1978); S. P. Mikheev and A. Y. Smirnov, *Sov. J. Nucl. Phys.* **42**, 913 (1985) [*Yad. Fiz.* **42**, 1441 (1985)].
- [17] A. Friedland, *Phys. Rev.* **D64**, 013008 (2001).
- [18] S. Mansour and T. K. Kuo, *Phys. Rev.* **D58**, 013012 (1998), hep-ph/9711424.
- [19] J. N. Bahcall, M. C. Gonzalez-Garcia, and C. Peña-Garay, *JHEP* **07**, 054 (2002), hep-ph/0204314.
- [20] J. N. Bahcall, M. C. Gonzalez-Garcia, and C. Peña-Garay, *JHEP* **02**, 009 (2003), hep-ph/0212147.
- [21] B. T. Cleveland *et al.*, *Astrophys. J.* **496**, 505 (1998).
- [22] J. N. Abdurashitov *et al.* (SAGE), *J. Exp. Theor. Phys.* **95**, 181 (2002), astro-ph/0204245.
- [23] W. Hampel *et al.* (GALLEX), *Phys. Lett.* **B447**, 127 (1999).
- [24] T. Kirsten, talk at the XXth International Conference on Neutrino Physics and Astrophysics (NU2002).
- [25] S. Fukuda *et al.* (Super-Kamiokande), *Phys. Lett.* **B539**, 179 (2002), hep-ex/0205075.
- [26] Q. R. Ahmad *et al.* (SNO), *Phys. Rev. Lett.* **87**, 071301 (2001), nucl-ex/0106015.
- [27] Q. R. Ahmad *et al.* (SNO), *Phys. Rev. Lett.* **89**, 011301 (2002), nucl-ex/0204008.
- [28] Q. R. Ahmad *et al.* (SNO), *Phys. Rev. Lett.* **89**, 011302 (2002), nucl-ex/0204009.
- [29] S. N. Ahmed *et al.* (SNO) (2003), nucl-ex/0309004.
- [30] J. N. Bahcall and M. H. Pinsonneault (2004), astro-ph/0402114; <http://www.sns.ias.edu/~jnb>.
- [31] K. Eguchi *et al.* (KamLAND), *Phys. Rev. Lett.* **90**, 021802 (2003), hep-ex/0212021.
- [32] N. Fornengo, M. Maltoni, R. T. Bayo, and J. W. F. Valle, *Phys. Rev.* **D65**, 013010 (2002), hep-ph/0108043.
- [33] M. Guzzo *et al.*, *Nucl. Phys.* **B629**, 479 (2002).
- [34] P. C. de Holanda and A. Y. Smirnov (2003), hep-ph/0307266.
- [35] A. Friedland and C. Lunardini, *Phys. Rev.* **D68**, 013007 (2003); *JHEP* **10**, 043 (2003).
- [36] Among other reasons, the processes changing the flavor of the background fermion do not add up coherently [35].
- [37] It has been proposed to detect pep neutrinos by electron scattering (M. Chen, private communications) or by CC absorption (R. S. Raghavan, talk at NOON04, Japan).